Improved understanding of the pozzolanic behaviour of MSWI fly ash with $Ca(OH)_2$ solution

Athanasius P. Bayuseno*

Department of Mechanical Engineering,
Diponegoro University,
Campus Tembalang, Semarang, 50255, Indonesia
Email: apbayuseno@gmail.com
*Corresponding author

Wolfgang W. Schmahl

Department of Geo-and Environmental Science,
Ludwig-Maximilians University of München, Germany
Email: wolfgang.schmahl@lrz.uni-muenchen.de

Abstract: The study aims at investigating pozzolanic behaviour of MSWI fly ash in a saturated $Ca(OH)_2$ solution at various times. The raw and water-washed fly ashes were selected for the pozzolanic solidification experiment to which mass ratios of the solution to ash (ml/g) were adjusted to be 3 and 10, whereas the solidification times were set from 7 to 28 days and from one to three months. From the XRD Rietveld analysis, a mineral assemblage of fly ash exhibited pozzolanic reactivity to form compounds of hydraulic cementitious materials. Here the considerable amounts of syngenite and gypsum, but small amounts of ettringite, hydrocalumite and C-S-H phase, were produced during the pozzolanic reaction of raw fly ash. Likewise, the washed fly ash exhibited the cementitious property with high quantity of gypsum and ettringite. From the leaching test, the solidified products exhibited release of lesser heavy metals about the untreated parent materials.

Keywords: pozzolanic solidification; MSWI fly ash; cementitious property; Rietveld analysis; mineralogical analysis.

Reference to this paper should be made as follows: Bayuseno, A.P. and Schmahl, W.W. (2015) 'Improved understanding of the pozzolanic behaviour of MSWI fly ash with $Ca(OH)_2$ solution', *Int. J. Environment and Waste Management*, Vol. 15, No. 1, pp.39–66.

Biographical notes: Athanasius P. Bayuseno is a Professor in Materials Science and Engineering and Head of Graduate Program in Mechanical Engineering at the Diponegoro University. He received his BSc in Mechanical Engineering from Gadjah Mada University, Indonesia, MSc in Applied Physics from Curtin University Australia and PhD in Mineralogy from Ruhr University of Bochum, Germany. His teaching interests are in ceramics, materials science and engineering. His research interests cover many aspects of ceramics design, applied crystallography including the materials characterisation and waste processing.

Wolfgang W. Schmahl is a Professor of Inorganic and Biogenic Materials at the Ludwig-Maximilians-Universität (LMU) Munich, Germany and Director of the Mineralogischen Staatssammlung Munich. His research interests are applied crystallography, nanoscience and computational materials science. He has published more than 100 research papers in journals.

1 Introduction

In Germany, municipal solid waste (MSW) is commonly incinerated and incineration residues are disposed in landfill. The MSW incinerated rate is reported about 37% or 220 kg per capita. MSW incineration (MSWI) has the advantage to reduce MSW weight and volume in addition to recovering some of the high calorific value of waste for generating electricity and steam. However, the incineration generates

1 a large quantity of bottom ash consisting of a slag-type material, containing metallic pieces and unburned materials

2 air pollution control (APC) residues including fly ash and acid gas scrubbing residues containing substantial amounts of heavy metals (i.e., Cd, Cr, Cu, Hg, Ni, Pb and Zn) as well as trace amounts of organic pollutants (polychlorinated dibenzo-p-dioxins and furans-PCDD/F) (Hjelmar, 1996; Sabbas et al., 2003).

In particular, a large amount of bottom ash has been recycled commonly in Germany as a secondary building material for civil engineering applications. However, the potential leachability of heavy metals and toxic organic components of fly ash are still a major concern in many countries regarding to environmental acceptability as a landfill deposit or as a resource (Akiko et al., 1996; Le Forestier and Libourel, 1998). Accordingly, fly ash must be treated to make it more acceptable for land disposal or recycling it in the concrete manufacturing both as aggregates or mineral additions (Ferreira et al., 2003).

The hazardous fly ash is frequently treated in cementitious, organic or vitreous matrix, physical/chemical of separation and then disposed of in landfills (Alba et al., 2001; Hong et al., 2002a, 2002b; Katsuura et al., 1996; Park and Heo, 2002; Polettini et al., 2004; SØrensen et al., 2000). The commonly used method is stabilisation and solidification (S/S) of fly ash with Portland cement into stable complexes (Aubert et al., 2006; Erol et al., 2001; Yvon et al., 2006, 2008). For a long time, this method has been known as an economical option for the waste management strategy to which toxic components are incorporated in a cement matrix through either physical or chemical immobilisation mechanisms, depending on the particular contaminant to be fixed and binder being used. However, the solidification with Portland cement presents some disadvantages. Specifically, protection against humidity is required to prevent breakdown and leaching of heavy metals. Numerous studies have demonstrated that the hydrated Portland cement paste is a moisture-sensitive material, i.e., that many of its physical, mechanical and chemical properties other than the hydration process itself are humidity dependent (Malviya and Chaudhary, 2006). In addition, salts present in fly ash interfere

with basic hydration reactions of cement, leading to an inadequate set deterioration of the waste form over time (Ubbriaco and Calabrese, 2000).

Pozzolanic solidification of fly ash in a solution enriched with $Ca(OH)_2$ to take an advantage of the pozzolanic property is an attractive method to help handling and reduce toxicity before landfill (Ubbriaco et al., 2001). MSWI fly ash may be pozzolan, because it is known to be rich in amorphous silica and alumina and becomes cementitious if combined with an activator (*lime*, or *Portland cement*) in the presence of water (ACI 116R, 2000; Quina et al., 2008). Here formation of the cementitious material is mainly controlled by the mass ratio of water to fly ash (Glasser, 1997) and depends greatly on the pozzolanic reactivity where the reactive compounds (e.g., SiO_2, Al_2O_3, CaO, and Fe_2O_3) of fly ash play a major role (Bertolini et al., 2004; Pan et al., 2008). Mineralogical phases of the reactive components subsequently react with water through dissolution-diffusion-precipitation processes resulting in the different hydrated phases such as ettringite, gypsum and hydrocalumite. Additionally, an amorphous calcium silicate hydrate (C-S-H), gehlenite hydrate (C_2ASH_8), calcium aluminate hydrate (C_4AH_{13}) and sometimes calcium carbo-aluminate are to be easily formed using $Ca(OH)_2$ an activator. The formation of the secondary mineralogical phases eventually provides a good degree of stabilisation of the hardened fly ash. This stabilised fly ash becomes, in principle, more compatible for storage, landfill or reuse as a resource.

Further, pozzolanic solidification of fly ash is believed to be the mainly promising way to provide a positive result of heavy metals retention in the hydrated phases (e.g., ettringite, gypsum and hydrocalumite) and glassy matrices (e.g. amorphous C-S-H), thereby minimising the heavy metal leachability (Cornelis et al., 2008). The amorphous phases have been known to be reactive sorptive minerals being able to fix hazardous elements Cd, Zn, Cu, Pb and Mo. However, these phases are thermodynamically unstable at ambient temperature and subsequently transform into more crystalline phases with different binding capacity for the heavy metals, depending on the structural constraints of the ordered phases (Aubert et al., 2007; Chen et al., 2009). Moreover, the pozzolanic and hydration reactions involving minerals of fly ash remain poorly understood and lack quantification until now (Williams et al., 2002; Mahieux et al., 2010). Here, the pozzolanic property of fly ash in the atmospheric condition depends on the chemical and mineralogical composition, the type and proportion of its active phases, the particle's specific surface area, the ratio of lime to fly ash, water content, curing time and temperature (Quina et al., 2008; Walker and Pavıa, 2011). Furthermore detailed knowledge of mineralogical compositions of fly ash and the solidified product is required to examine the correlation of both the microstructure (crystalline and glassy phases) and the solidification parameter and thus, to optimise pozzolanic property of fly ash.

The present study was undertaken to examine pozzolanic property of MSWI fly ash in the saturated $Ca(OH)_2$ solution and the degree of reactivity for their minerals. The emphasis of this study was to gain some insight into secondary minerals for controlling the pozzolanic behaviour of fly ash. The degree of amourpheness of the microstructure influencing the activity of pozzolan was analysed by the Rietveld refinement method for X-ray diffraction (XRD). The toxicity characteristic leaching procedure (TCLP) was for testing the hazardous fly ash and the solidified products.

2 Experiments

2.1 Materials

Samples of MSWI fly ash were collected from the electrostatic precipitator (ESP) facilities at an incinerator plant in the town of Iserlohn close to the Ruhr industrial area, Germany (for our study we did not average samples taken over a longer time period). It is assumed that this residue constitutes representative samples of the MSWI fly ashes generated by acid gas scrubber using a liquid spray and dust filter. Part of the sampled fly ash was then homogenised within 24 hours after sampling with an agate vibratory disc mill for 30 minutes, until all material had passed a 100 μm sieve. Use of fine particle size powders was regarded important to enhance the pozzolanic activity. The ground material was then kept in an open bucket in the laboratory under 'dry' conditions (typically 60–70% relative humidity) until analysis. This material is referred to as 'raw fly ash' for the experimental study.

Furthermore, the water-washing treatment of fly ash was conducted for extracting soluble salts and minimising heavy metal leachability (Mulder, 1996; Wang et al., 2001). As a consequence of the high release of water-soluble compounds and the low release of heavy metals, all washed fly ash residues tend to be enriched in heavy metals (Cd, Cr, Cu, Ni, Pb and Zn), thereby yielding a potentially hazardous material. However, the removal of chlorides from the fly ash may be beneficial for the fixation of heavy metals through immobilisation processes in the cementitious material, because salts (mainly chlorides) in the fly ash will negatively interfere with the solidification of fly ash material. A number of elements (Ca, Si, Al, P, Mg and Fe) also tend to increased weight percentage due to the diluting effect of water-soluble compounds (Cl-, Na and K). The pre-treatment stage benefits of fly ash by the washing procedure were somewhat offset by generating a new waste residue containing chlorides, water-soluble sulphate and alkali ions (Wang et al., 2001; Sabbas et al., 2003). Hence, a degree of compromise was involved in the selection of the pre-washing treatment because of the competition concerning quality benefits of the fly ash for subsequent treatment and producing other pollutants. However, it was envisaged that the pozzolanic reactivity of fly ash is to be improved by such a pre-treatment due the less influence of salts as proposed by Mangialardi (2003).

The water-washing treatment of fly ash was conducted in a glass beaker equipped with a magnetic stirrer for mixing at 300 rpm. Batches of 70 grams of the fly ash powder were prepared. Batches were initially placed in the glass beaker containing deionised water. The water to the solid mass ratio (ml/g) was set to 10. The pH obtained for this mixture is between 10 and 11. Subsequently, this mixture was stirred to stand for 24 hours at room temperature. At the end of stirring, the resulting slurries were filtered with a paper filter (Schleicher&Schuell No. 604), washed repeatedly with deionised water, and dried at room temperature for subsequent material characterisation and solidified experiments. This is referred to as the 'washed fly ash' material of our study.

Table 1 Bulk chemical composition of raw and washed fly ashes

Element	*Raw fly ash*	*Washed fly ash*
	wt.%	
Al	2.43 (02)*	3.73 (06)
Ca	12.41 (22)	18.97 (26)
Cl	8.32 (14)	0.56 (0)
Fe	3.71 (05)	3.99 (08)
K	6.11 (08)	0.99 (01)
Mg	1.08 (02)	1.57 (04)
Mn	0.12 (0)	0.18 (02)
Na	10.38 (28)	3.09 (07)
P	0.40 (0)	0.55 (0)
Pb	1.36 (07)	2.17 (09)
S	4.12 (0)	5.49 (0)
Si	5.63 (20)	6.95 (25)
Ti	1.02 (02)	1.53 (05)
Zn	4.91 (03)	8.09 (08)
LOI	8.51 (28)	
	ppm	
As	307 (25)	1,029 (30)
Ba	3,470 (93)	5,365 (75)
Bi	204 (2)	364 (5)
Cd	456 (6)	751 (7)
Co	262 (18)	265 (19)
Cr	2,026 (29)	2,924 (39)
Cs	114 (3)	184 (5)
Cu	3,513 (32)	5,660 (24)
F	1 (0)	5,131 (28)
Ga	3,042 (229)	43 (0)
Mo	30 (4)	609 (4)
Ni	9 (1)	799 (21)
Rb	34 (1)	27 (2)
Sb	3 (0)	2,678 (2)
Sn	489 (7)	557 (8)
Sr	24 (4)	744 (6)
V	614 (19)	122 (14)
Y	6 (3)	1,436 (24)
Zr	265 (3)	336 (7)

Notes: LOI = loss on ignition; *figures in parentheses indicate the estimated standard deviation (esd) reference to the least significant figure to left. A zero indicates an esd < 0.001%.

2.2 Bulk chemical analysis

Total elemental composition of fly ash (mass of element/dry mass of ash) was conducted by wavelength dispersive (WDS) X-ray fluorescence (XRF) with lower detection limits (LDL)-down to a few ppm (order of not as much of 10 ppm) for all size fractions (< 100 μm) of the fly ash materials. Further, batches of 8 grams of the sample were mixed with 2 g of acetone as a binder. The acetone was employed to increase densification. The mixture was finely homogenised in an agate bowl. The powder pellets were subsequently pressed at 20 kg/cm^2 for 2 minutes and finally analysed by XRF for all elements present in the ash, except for any elements with atomic mass < 19. Loss on ignition (LOI) was determined according to ASTM C 25 by heating fly ash to constant mass at 750°C. The bulk chemical compositions of the raw and washed fly ash powders were determined by WDS XRF.

2.3 XRD characterisation

The raw, washed and solidified fly ash was subjected to XRD analysis. Each sample was ground for 10 min with a mortar and pestle. Finally, the powder of each specimen was loaded into a plastic or aluminium sample holder, and subsequently flattened and compacted with a glass slide.

XRD analysis was done on a conventional Bragg-Brentano (BB) parafocusing geometry (Siemens D500 and Philips X-Pert Diffractometer) using Cu-Kα monochromated radiation. The accelerating voltage was 45 kV, and the current was 30 mA. The scan parameters (5–85° 2θ in 0.020° increments, 10–15 s/step) were selected as required for observation. Data were recorded digitally, and peak positions and intensities were identified by using the peak search finder feature or on screen in the software. A PC-based search match program, the Philips X'Pert Software (Philips Electronics N.V) involving the Joint Committee of Powder Diffraction Society (JCPDS) database as a source of reference data was employed to help the identification of the possible crystalline phases in the ash samples. The 'possible' crystalline phases candidates suggested by search match procedures were subsequently judged by the Rietveld full profile fitting analysis in parallel to the subsequent quantitative phases analysis of the material (Rietveld, 1969). The Rietveld method was selected for our study because:

1 quantitative information for minor phases was desired
2 significant (sometimes total) overlapping peaks were present in samples
3 best confidence in the reliability of result was desired as proposed by Mahieux et al. (2010).

The wt. % levels of mineralogical phases including the glass content were determined by the XRD Rietveld analysis using an internal standard method (Hill and Howard, 1987). In this case, the selected fly ash sample was initially mixed with 10 wt. % of CeO_2 (NIST SRM 674) as internal standard. The CeO_2 powder was assumed to be fully crystalline. The Rietveld calculations were done using the SIROQUANT (2002) *Quantitative XRPD software* program. The SIROQUANT contains an extensive database of crystal structure models from which the full diffraction profiles are calculated. Additional structure models were taken from the Inorganic Crystal Structure Database

(ICSD, 1999). Detailed discussion of the calculation method is presented elsewhere (Bayuseno, 2006). The abundances of both the raw and washed fly ashes, estimated from powder XRD traces using the Rietveld refinement method, are presented in Table 2.

Table 2 XRD-based mineralogy of the raw and washed fly ashes

Mineral phase (wt. %)	*Formula*	*Raw fly ash*	*Washed fly ash*	*Structure model§*
Amorphous		57.4(9)*	47.2(6)	
Albite (plagioclase)	$NaAlSi_3O_8$	1.1(2)	6.3(3)	S-155
Alunite	$NaKAl_3(OH)_6(SO_4)_2$	1.4(1)		S-459
Anhydrite	$CaSO_4$	4.5(3)	5.2(1)	S-80
Apatite	$Ca_5(PO_4)_3OH$	2.0(2)		S-215
Augite	$Ca_3Na_3Mg_3FeAl_{1.6}Si_7O_{24}$		1.7(2)	S-622
Bassanite	$CaSO_4 \cdot 0.5H_2O$	0.7(1)		S-292
Calcite	$CaCO_3$	1.7(2)	3.3(1)	S-11
Caracolite	$Na_3Pb_2(SO4)_3Cl$	0.4(1)		I-024459
Calcium titanite	$CaTiO_3$	0.4(1)		S-757
C_3A	$Ca_3Al_2O_6$	0.9(1)	0.6(1)	S-71
C_2S	Ca_2SiO_4	0.8(1)	0.7(2)	S-69
C_3S	Ca_3SiO_5	0.9(2)	0.8(2)	S-128
Diopside	$CaMgSi_2O_6$	1.8(2)		S-133
Enstatite	$(Mg, Fe)SiO_3$	1.2(2)		S-151
Ettringite	$3CaO \cdot Al_2O_3 \cdot 3CaSO_4 \cdot 32H_2O$		1.4(1)	S-195
Forsterite (olivine)	$(Mg,Fe)_2SiO_4$	2.0(2)		S-53
Hydro-garnets	$Ca_3(Al,Fe)_2(Si,P)_3O_{12}$	0.4(1)		S-552
Gehlenite (melilite)	$(Ca,Na)_2(Mg,Fe,Si,Al)_3O_7$	1.4(2)	2.9(1)	S-165
Gordaite	$NaZn_4(SO_4)(OH)_6Cl(H_2O)_6$		0.5(1)	I-406090
Gypsum	$CaSO_4 \cdot 2H_2O$		16.4(2)	S-355
Halite	NaCl	5.3(1)		S-105
Hematite	Fe_2O_3	1.8(1)	0.8(1)	S-41
Hydrocalumite	$Ca_8Al_4(OH)_{24}(CO_3)(Cl)\ (H_2O)_{9.6}$	0.7(1)	2.1(1)	S-778
Illite	$KAl_3Si_3O_{10}(OH)_2$	0.4(0)		S-116
Iron	Fe	0.5(1)		S-140
Kalsilite	$KAlSiO_4$	0.3(0)	1.9(0)	S-961
Lepidocrocite	FeOOH		0.6(1)	S-45
Marcasite	FeS_2		0.4(1)	S-362
Minium	Pb_3O_4	0.8(1)	0.3(0)	S-713
Magnetite	Fe_3O_4	0.9(1)	1.5(1)	S-50
Nepheline	$Na_3KAl_4Si_4O_{16}$	1.2(2)	1.0(1)	S-89

Notes: *Figures in parentheses indicate the least-squares estimated standard deviation (esd) reference to the least significant figure to left, a zero indicates an esd < 0.05%.
§The reference is given as a letter S for the SIROQUANT (2002) database and I for the ICDD followed by the entry number of the respective database.

Table 2 XRD-based mineralogy of the raw and washed fly ashes (continued)

Mineral phase (wt. %)	*Formula*	*Raw fly ash*	*Washed fly ash*	*Structure model§*
Portlandite	$Ca(OH)_2$	0.4(1)		S-124
Pyrite	FeS_2	0.5(1)		S-29
Quartz	α-SiO_2	1.5(1)	2.0(1)	S-1
Rutile	TiO_2	0.9(1)	0.7(1)	S-15
Sanidine	$KAlSi_3O_8$	2.0(3)		S-21
Sodalite	$Na_4Al_3Si_3O_{12}Cl$	0.4(1)	0.5(1)	S-1031
Sylvite	KCl	1.2(1)		S-164
Tobermorite-14 Å	$Ca_5(OH)_2SiO_{16}{\cdot}4H_2O$	0.5 (1)		S-309
Ulvöspinel	Fe_2TiO_4	0.9(1)	1.2(1)	S-362
Zinc Chloride	$ZnCl_2$	0.8(0)		S-5
	Total	100	100	

Notes: *Figures in parentheses indicate the least-squares estimated standard deviation (esd) reference to the least significant figure to left, a zero indicates an esd < 0.05%.
§The reference is given as a letter S for the SIROQUANT (2002) database and I for the ICDD followed by the entry number of the respective database.

2.4 Complementary analytical methods

The raw fly ash was characterised by optical polarisation microscopy (LEICA) and electron micro-probe analysis (EPMA) to explore the mineralogical phase compositions within the individual particles. Examinations of thin sections using polarisation microscopy and EPMA provided a generalised understanding of minerals that are present in the raw fly ash. These procedures were also used to check on consistency of our analysis, but in some cases allowed identification of phases which were not found by XRD. .Microprobe analyses using a CAMECA SX50 operating in WDS mode were selected to confirm the XRD results for the mineralogical characterisation of fly ash. Here backscattered electron (BSE) image was used for discrimination of phases based on mean atomic number. For the investigation, the fly ash particles were separated by manual sieving and subsequently embedded in epoxy matrix on a glass slide with a size of 48 mm × 28 mm × 1.0 mm, and polished with a final diamond powder grain size of 1 μm. The specimens were finally mounted onto aluminium stubs using double-sided adhesive carbon discs and sputter coated with gold for subsequent quantitative analyses.

The quantitative analyses were done at 15 keV and 2–10 nA using either a defocused electron beam of 5 or 10 μm spot size or a rastered beam at 20,000–40,000 times magnification. The conventional ZAF correction method (Z = atomic number, A = absorption factor, F = characteristic fluorescence correction) was used and this method is based on the peak-to-background method (P/U-ZAF correction). Elements with Z < 11 such as H, C, and O may not be spectroscopically determined on the (and mainly other) WDS systems, but oxygen content was determined by stoichiometry. The counting time of 6 seconds was selected for the major elements, and subsequently was increased to 20 seconds for trace metals. The mineral standards employed were albite ($NaAlSi_3O_8$) for Na Kα and Si Kα; orthoclase ($KAlSi_3O_8$) for K Kα; Al_2O_3 for Al Kα; $MnTiO_3$ for Ti Kα

and Mn Kα; andradite [$Ca_3Fe_2(SiO_4)_3$] for Ca Kα; Fe_2O_3 for Fe Kα; forsterite (Mg_2SiO_4) for Mg Kα; Cr_2O_3 for Cr Kα; FeS2 for S Kα; metal Cu for Cu Kα; ZnO for Zn Kα and bao for Ba Kα. Matrix effects corrections were made with the 'PAP' program (Pouchou and Pichoir, 1991). H_2O or OH contents were calculated by the assumed mineral formula stoichiometry and the experimentally determined relative concentrations of the measured cations. Here the obtained sum of weight percentages in the calculative models deviated from 100%. If the deviation was small, the assumptions were believed to be correct. However, in the present paper analyses of hydrated minerals were not provided.

Further, the solidified materials were investigated by scanning electron microscopy (SEM) on a LEO DSM apparatus equipped with an EDS for characterising the microstructure and morphology. For the observation, the solidified product was ground for 10 min with a mortar and pestle, and then embedded in epoxy on a glass slide with a size of 48 × 28 × 1.0 mm and finally polished with a final diamond powder grain size of 1 μm.

2.5 Pozzolanic solidification experiment

The pozzolanic activator selected was $Ca(OH)_2$ powder with p.a. grade supplied by Merck, Germany. Saturated solution of $Ca(OH)_2$ was prepared by dissolving $Ca(OH)_2$ powder in a glass beaker containing distilled water with molar ratio = 0.185 g/100 cm^3. A magnetic stirrer was employed for mixing the slurry at 300 rpm for 24 hours. The beaker was opened to ensure aerobic conditions (i.e., available oxygen and CO_2 amount and good diffusion of oxygen in the sample). The solutions were then centrifuged and filtered through a paper filter (Schleicher&Schuell No. 604). Here, the saturated solution was to be selected for subsequent pozzolanic solidification of fly ash specimens.

Solidified materials were prepared by mixing fly ash with the saturated solution. For this purpose, two different kinds of fly ash were employed:

1 the raw fly ash

2 the water-washed fly ash.

The solution with liquid to fly ash mass ratio, hereinafter referenced to as L/S (liquid/solid) mass ratio, was adjusted to be 3:1 and 10:1 (ml/g). This approach was considered to be of particular significance in order to promote a pozzolanic reaction between the amorphous silica in fly ash and $Ca(OH)_2$ available in the solution. The pH obtained when the raw and washed fly ashes mixed with the saturated solution was from 10 to 11. For obtaining the homogenous slurry, a mixture of fly ash-saturated solution was stirred at a constant speed of 300 RPM for 5 hours. At the allotted time periods, the resulting slurry was placed in an open plastic container in the laboratory air under dry conditions (typically 60–70% relative humidity) and then dried at room temperature. The samples with an L/S ratio of 3 were hydrated from 7 to 28 days; but the longer setting times (from one to three months) for samples with an L/S ratio of 10 were selected for obtaining the solidified products. The container was opened from time to time to admit fresh air and thus maintained aerobiosis throughout solidification. At the end of the pozzolanic solidification experiment, the dried cake products were crushed and stored within a plastic container until analysis.

2.6 Leaching test

Leaching tests were done according to the standard of the TCLP of the Environmental Protection Agency (U.S. EPA, 1990) (EPA-SW 846 Method 1311). 5 g of the powder batches (raw, washed and solidified fly ashes) were initially ground to particles less than 100 μm in size. In this method, the ground sample was subsequently extracted by using an acetic acid solution (CH_3COOH) supplied by J.T. Beaker, (Holland) mixed with distilled water. Here, the acetate buffer was added once to have a solution with a pH of 3, at the beginning of the extraction. The tested sample was first placed in a glass beaker containing the acetic acid solution and stirred in the magnetic stirrer at 300 RPM. The solution with a liquid-to-solid mass ratio of 20:1 (ml/g) was selected and the time of extraction was 18 ± 3 h. After the leaching process, the leachants were filtered through a paper filter (Schleicher&Schuell No. 604) and pH was again measured before conducting chemical analysis. The concentrations of heavy metals in the leachants were determined by inductively coupled plasma mass spectroscopy (ICP-MS).

3 Results

3.1 Microscopic characterisation of raw fly ash

Under the BSE (back scattered electron) images, the raw fly ash revealed spherical particles, either hollow (cenospheres) or filled, or exhibited a series of smaller spheres (plerospheres). The spherical particles were obviously composed of calcium aluminosilicate as indicated by WDS spectra. Similar spherical aluminosilicate morphologies found in the MSWI fly ash have been also reported by Eighmy et al. (1995).

In the present study, BSE imaging of the polished thin sections obtained by electron probe microanalysis at several spots was used to correlate the different mineralogical phases with the different morphologies. The analysis of up to 181 punctual spectra was taken to localise the different trace elements observed. Representative micro-probe analysis of minerals obtained from several WDS spectra at locations (spots-showed by the number) indicated on the BSE images are presented in Table 3. By WDS data, the mineral formula with or without oxygen were then recalculated according to a procedure described by Deer et al. (1996). Quartz and magnetite particles were mainly readily distinguished during this work. Quartz typically occurred in the spherical or rounded area was also observed (see Figure 1). Amounts of metallic aluminium and silicon particles within silicate agglomerates were also identified.

Among spherical particles are glasses that have a silicate-rich aluminosilicate composition, but many of these spheres contain considerable amounts of calcium as well (Table 3; spots of 11 and 18). The presences of glassy phases in the fly ash were to be directly observed under the optical microscope. The typical glasses with a calcium-rich aluminosilicate composition found in fly ash are similar to those previously observed by Le Forestier and Libourel (1998). A large compositional variation of different irregular shapes of particles was also investigated. The mainly prominent characteristic of these particles was the abundance of FeO (Table 3), but some of these particles contain calcium and silica as well. The composition of some particles approaches that of Fe-rich garnet close to the structural formula $(Ca_{2.5}Mg_{0.5}Fe^{+2}_{0.2}Zn_{0.01})(Al_{0.9}Fe^{+3}_{0.9}Ti_{0.16})$

$(Al_{0.2}P_{0.64}Ti_{0.04}Si_{2.1})O_{12}$. But it may be hydro-garnets [M3II, M2III(SiO_4)(3-x) (OH)4x], where MII and MIII are respectively bivalent and trivalent metals. Additionally, iron-bearing pyroxene with formula $(Ca_{0.13}Na_{0.21}K_{0.15}Fe^{total}_{0.85}Mg_{1.2})(Al_{0.2}Si_{1.8})O_6$ had been observed. Several Ca-Al-sulphates, possibly ettringite, chlorides and complex silicates were also recognised. Some of these phases present in fly ash were also confirmed by XRD Rietveld method (Table 2).

The large compositional ranges of WDS data for several particles were thus being classified by group of minerals, i.e., silicates, alloys, chlorides, sulphates, phosphates and oxides. For major elements Ca, Na, K, Fe, Al, Si and O, the following crystalline phases identified are alkali feldspar, melilite group to akermanite-gehlenite, olivine to fayalite, plagioclase to anorthite-albite. The alkaline feldspars as determined by WDS could be any potassic feldspar, sanidine, orthoclase, adularia or microcline. Moreover, alloys for metallic phases consisted of zinc, iron, aluminium, nickel and chromium. These alloys were not detected by XRD; they are probably present at low concentration. It may occur that the 1.99 Å reflection of halite overlaps the 2.00 Å reflection of many metals, occulting them if they are in small amounts. Microprobe analyses also allowed the identification of anhydrite and apatite in addition to many complex sulphate minerals; but the mineral oxides of fly ash were dominated by rutile, lime and escolaïte (Cr_2O_3). Several calcium-containing minerals including $CaAl_2O_4$, hatrurite (Ca_3SiO_5) and wollastonite $(CaSiO_3)$ were observed. Specifically, the magnetic fraction consisting of hematite and magnetic-spinel were identified and analysed quantitatively. Similar observations have been also reported by previous researchers for a comparable particles fly ash (Eighmy et al., 1995; Le Forestier and Libourel, 1998).

Further WDS data revealed detectable concentrations of several trace metals in the fly ash particles. A complex distribution of pollutant elements (Cd, Cr, Ni, Pb, Zn) was observed, although the elements are not shown in the present paper. Cd-bearing mineral was not detected, probably present amorphous phase. Additionally, Cr and Ni were identified; and were probably present as metal and in complex silicates and oxides. Subsequently, complex distribution of Pb was found as soluble salts, as metal, and in sulphates, silicates and oxide. Zinc, the mainly abundant pollutant element, was found possible alloys, chloride, sulphates, spinels and calcium-bearing aluminosilicates glasses. Apparently Ca-rich and S-rich phases represent as an important host for trace elements such as Pb and Zn (Eighmy et al., 1995; Le Forestier and Libourel, 1998).

3.2 Formation of hydrated phases during solidification of raw fly ash

Major crystalline phases in the raw fly ash are anhydrite (An), gehlenite (G), halite (Hl) and sylvite (S) in addition to minor minerals such as alunite (Al), bassanite (Ba), calcite (C), hydrocalumite (Hc), portlandite (Po) and ulvöspinel (Us) [Figure 2(a)]. The formation of minerals namely bassanite and hydrocalumite in the raw fly ash may be due to aging during storage at the laboratory. The formation of Ca-Al-SO_4^{2-}-Cl-hydrate phases (e.g., hydrocalumite) is likely initiated by dissolution of Ca-Cl-and Al-rich minerals. Much of amorphous material (> 50 wt. %), probably Ca-rich aluminosilicate glasses play an important role in pozzolanic solidification of fly ash (Tables 2 and 3).

Table 3 Electron microprobe analyses of MSWI fly ash (chemistry given in weight % of oxides)

Spot	*Minerals*	Na_2O	*MgO*	Al_2O_3	SiO_2	P_2O_3	SO_3	*Cl°*	K_2O	*CaO*	TiO_2	Cr_2O_3	*FeO*	*NiO*	*CuO*	*ZnO*	*CdO*	*SnO*	*BaO*	*PbO*	*Total*
1	Pyroxene	2.23	4.34	12.31	33.48	0.35	0.06	0.09	0.08	37.72	2.99	0.08	3.37	0.13	0.05	2.01	0.05	0.03	0.06	0.00	99.42
2	Quartz	0.00	0.02	0.00	99.90	0.03	0.01	0.04	0.03	0.08	0.00	0.04	0.01	0.00	0.00	0.01	0.00	0.00	0.19	0.00	100.34
3	Chloride	0.03	0.00	0.01	0.03	0.03	0.01	5.78	0.04	0.02	0.00	0.00	0.04	0.03	0.02	0.19	0.05	0.00	0.00	0.67	5.66
4	Ca-Al-Si-SO_4	0.25	1.09	3.17	11.65	0.28	20.16	3.16	1.51	28.95	0.42	0.06	0.50	0.02	0.00	13.19	0.21	0.01	0.09	0.00	84.00
5	[a]Garnet	1.21	1.72	9.60	21.80	7.81	0.31	0.08	0.60	25.17	2.65	0.08	20.39	0.18	0.15	0.14	0.08	0.02	1.45	0.00	93.43
6	Ca-Ba-Fe-Si-O	1.06	1.34	4.29	26.18	1.66	0.10	0.06	0.20	20.49	8.30	0.03	10.93	0.05	1.54	0.65	0.00	0.04	18.26	0.40	95.56
7	Ca-Fe-Si-O	0.02	5.96	2.27	2.44	0.15	0.16	0.01	0.05	2.35	2.16	0.49	63.98	0.66	4.39	3.60	0.07	0.13	2.01	0.00	90.89
8	Ca-Al-S-Cl-O	1.65	0.19	72.54	0.13	0.07	8.03	1.54	1.88	7.16	0.00	0.00	0.16	0.00	0.43	4.08	0.00	0.00	1.09	0.00	98.60
9	Ca-Al-S-Cl-O	0.24	0.54	30.41	0.64	0.05	13.55	5.86	1.74	19.32	0.00	0.05	0.14	0.08	1.10	3.25	0.11	0.01	4.00	1.34	81.11
10	Glass	4.64	4.90	15.20	36.83	3.33	0.06	0.04	0.91	18.78	1.71	0.02	9.27	0.06	0.21	0.67	0.06	0.07	0.33	0.14	97.23
11	Glass	0.64	2.71	8.07	27.21	2.53	4.08	0.08	0.20	45.71	0.34	0.09	4.11	0.01	0.25	1.20	0.00	0.07	0.00	0.00	97.29
12	Quartz	0.19	0.01	0.13	94.59	0.03	0.10	0.12	0.16	0.31	0.07	0.00	0.64	0.03	0.08	0.41	0.07	0.02	0.00	1.39	98.33
13	Garnet	1.09	0.80	7.85	24.59	0.75	0.04	0.03	0.25	15.12	1.95	0.13	42.63	0.04	0.16	0.48	0.08	0.07	0.32	0.01	96.39
14	Garnet	2.13	0.93	8.34	30.57	0.71	0.04	0.04	0.43	18.25	1.77	0.08	32.50	0.01	0.32	1.52	0.06	0.13	0.30	0.24	98.35
15	Ca-Fe-Si-Al-O	0.55	0.67	3.59	8.82	0.31	0.03	0.00	0.15	5.84	3.29	0.14	67.47	0.08	0.29	0.89	0.03	0.16	0.17	0.18	92.65
16	Glass	3.33	1.44	3.65	48.33	0.83	0.05	0.07	0.76	30.22	1.15	0.10	5.52	0.01	0.20	2.00	0.03	0.04	0.39	0.52	98.63
17	[b]Pyroxene	2.67	19.30	2.16	41.97	0.12	0.09	0.02	2.79	2.97	0.10	0.22	24.57	0.05	0.26	0.27	0.01	0.01	0.07	0.00	97.63
18	Glass	0.41	5.46	15.45	29.40	1.04	0.11	0.07	0.10	38.45	0.89	0.02	3.04	0.00	0.11	2.20	0.00	0.07	0.79	0.00	97.61

Notes: The spot numbers reference to Figure 1.
The composition of the observed minerals is presented as follows:
[a]Garnet: $(Ca_{2.5}Mg_{0.5}Fe^{+2}_{0.2}Zn_{0.01})(Al_{0.9}Fe^{+3}_{0.9}Ti_{0.16})(Al_{0.2}P_{0.64}Ti_{0.04}Si_{2.1})O_{12}$
[b]Pyroxene: $(Ca_{0.13}Na_{0.21}K_{0.15}Fe^{(total}_{0.85}Mg_{1.2})(Al_{0.2}Si_{1.8})O_6$

Figure 1 BSE micrograph of MSWI fly ash: polycrystalline aggregates having dimension to 50 μm with identified mineralogical phases

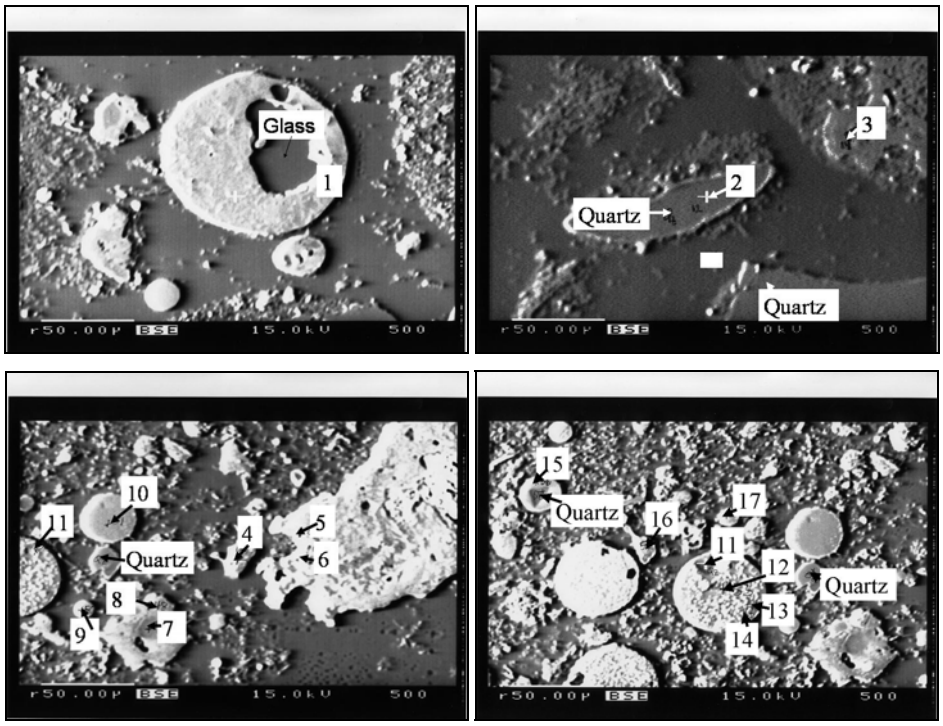

Note: The spot numbers refer to the numbers given in Table 3.

Figure 2(a) also presents XRD patterns of the secondary minerals for pozzolanic solidification at the L/S mass ratio of 3 and various times. Peaks corresponding to syngenite (Sy) [$K_2Ca(SO_4)_2 \cdot H_2O$] (PDF#74-2159), gypsum (Gy) ($CaSO_4 \cdot 2H_2O$) (PDF#70-0982) and ettringite (E) ($3CaO \cdot Al_2O_3 \cdot 3CaSO_4 \cdot 32H_2O$) (PDF#72-0646) were observed on the first seven days. All those hydrate phases are commonly found in the solidified products of Portland cement materials (Taylor, 1990). By increasing time (beyond seven days), a slow increase of the production of hydrate phases was observed, this is associated to the solidification of pastes. Here, the formation of a C-S-H mineral (Tb) (modelled by tobermorite-14 Å) with strongest peak at 7.76° 2θ, PDF#83-1520) was identified. Further, bassanite peaks disappeared; but a smaller reduction in peak intensities of anhydrite and sylvite was observed. Apparently, those minerals have undergone a base-induced dissolution process by providing compounds of Ca, K and SO_4 for the formation of hydrate phases. However, many phases such as calcite, quartz, and gehlenite exhibited a weak reactivity with the saturated $Ca(OH)_2$ solution. Typically, hydrocalumite present in the raw fly ash resisted during the solidification process, as indicated by the peak intensity of hydrocalumite persisting in all the XRD patterns.

Figure 2 XRD patterns of fly ash solidified with the saturated solution of $Ca(OH)_2$ using liquid/solid ratios of (a) L/S = 3 and (b) L/S =10 at various times

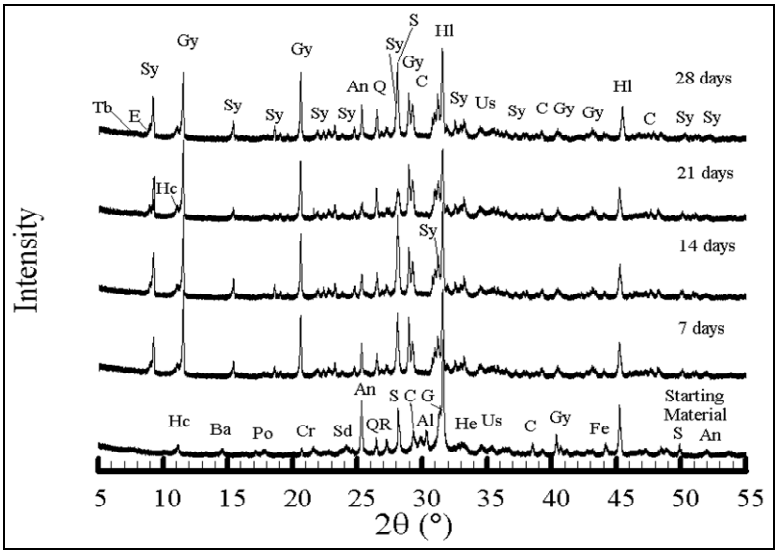

(a)

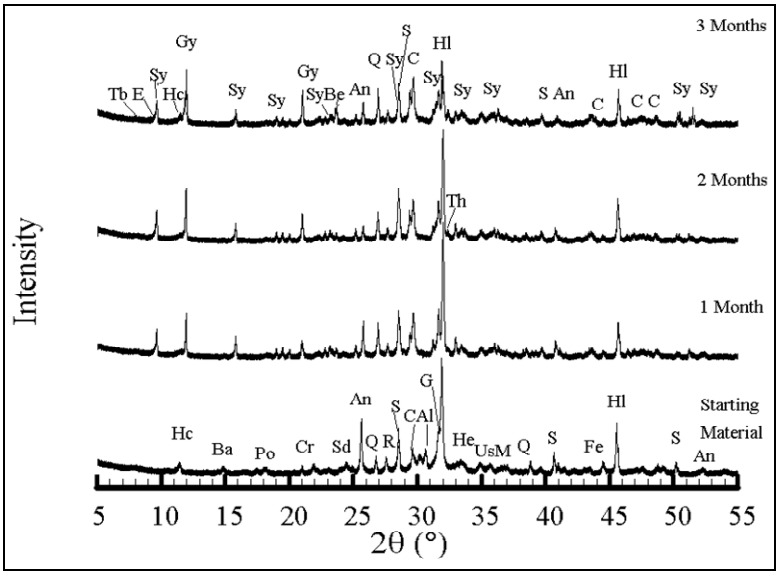

(b)

Note: The peaks are labelled Al (alunite), An (anhydrite), Ba (bassanite), Be (bernalite), C (calcite), Cr (cristobalite), E (ettringite), Fe (iron), Gy (gypsum), G (gehlenite), Hc (hydrocalumite), He (hematite), Hl (halite), M (magnetite), Po (portlandite), Q (quartz), R (rutile), S (sylvite), Sd (sodalite), Sy (syngenite), Us (ulvöspinel), Tb (tobermorite 14 Å-CSH phase) and Th (thenardite).

Likewise, the pozzolanic solidification of fly ash at the fixed L/S mass ratio of 10 for various times (one to three months) resulted in hydrate phases (i.e., syngenite and gypsum) [Figure 2(b)]. The XRD pattern of this solidified sample after three months showed a stronger peak of bernalite (Be) [$Fe(OH)_3(H_2O)_{0.25}$] at 23.57° 2θ (PDF#81-2022). But the overall pozzolanic reaction of fly ash greatly slowed down, in comparison with the experimental with the L/S ratio of 3. Anhydrite was converted slowly to gypsum. The disappearance of bassanite peaks and a significant reduction of peak intensities for halite in the solidified sample were also observed in XRD patterns. The formation of the C-S-H phases close to tobermorite-14 Å (PDF#83-1520) was also observed in all ages of the solidified sample. In the experiment with the L/S ratio of 10, ettringite was deserved just after 3 months. According to the previous work of Ubbriaco et al. (2001), the slow development of ettringite was associated with the lower concentration of aluminate and the low amount of portlandite in the solution.

The formation of syngenite on the solidified sample after 1 month at the L/S mass ratio of 10 was also confirmed by SEM/EDS analysis indicating syngenite of prismatic grains with 2–5 μm in diameter and the main elements of S, K, Ca, and O are shown in the EDS spectrum [Figure 3(a)]. This typical prismatic morphology is commonly found in the synthetic syngenite (Taylor, 1990). Moreover, the small amounts of Al, Na and Si in the EDS spectrum are probably the small grains on the surface of the prism grains [Figure 3(b)].

Mineralogical reactivity of raw fly ash during the pozzolanic solidification was evaluated quantitatively by the XRD Rietveld method [Figure 4(a)]. Hydrocalumite was initially formed; afterward the content remained roughly constant after course of the pozzolanic reaction. As the solidification proceeded, significant amounts of syngenite and gypsum (> 10 wt. %) were formed at times between 7–28 days. Syngenite is salt and it develops rapidly in the alkaline environment (Taylor, 1990). The high yields of syngenite and gypsum appeared to be associated with higher concentrations of Ca, K- and SO_4 in the parent material and those were largely provided by the glassy phase. But a little part of the chloride compounds interacts with the hydrate phases. Further, the highest quantities of syngenite (> 20 wt. %) and gypsum (>15 wt. %) were achieved at 28 days of solidification. In contrast, a low abundance of ettringite (< 2 wt.%) was produced. Moreover, the pozzolanic solidification of fly ash sample resulted in the small quantity of the C-S-H phase.

Further the pozzolanic solidification of fly ash sample at the L/S mass ratio of 10 for longer times (one to three months) clearly resulted in the reduction of syngenite content opposed by the increased content of gypsum [Figure 4(b)]. It appears that a significant quantity of sulphate from syngenite promoted the increased content of gypsum. Similarly, the contents of hydrocalumite and C-S-H phases are more likely to increase, but the abundance of glass reduces slightly.

The absence of any dramatic reduction of the glass content in this solidified sample in the L/S mass ratio of 10 is due to an excess of $Ca(OH)_2$ that forms a protective surface layer around glass particles, thereby leading the glassy phases to be stable during the pozzolanic reaction. Alternatively, a new stabilised glass is formed in the solidified product. Unexpectedly, the formation of ettringite was no longer found in pastes with the L/S mass ratio of 10. Hence, the L/S mass ratio is a key variable in the development of ettringite and C-S-H phases in the pozzolanic solidification of fly ash (Mangialardi et al., 1999; Ubbriaco et al., 2001). Supposedly, the smaller L/S mass ratios (< 3) are the more

promising result in the development of suitable solidification and stabilisation processes of fly ash.

Figure 3 (a) SEM image of prismatic crystals of syngenite and (b) EDX spectrum obtained from fly ash solidified with the saturated solution of $Ca(OH)_2$ at the L/S ratio of 10 for one month

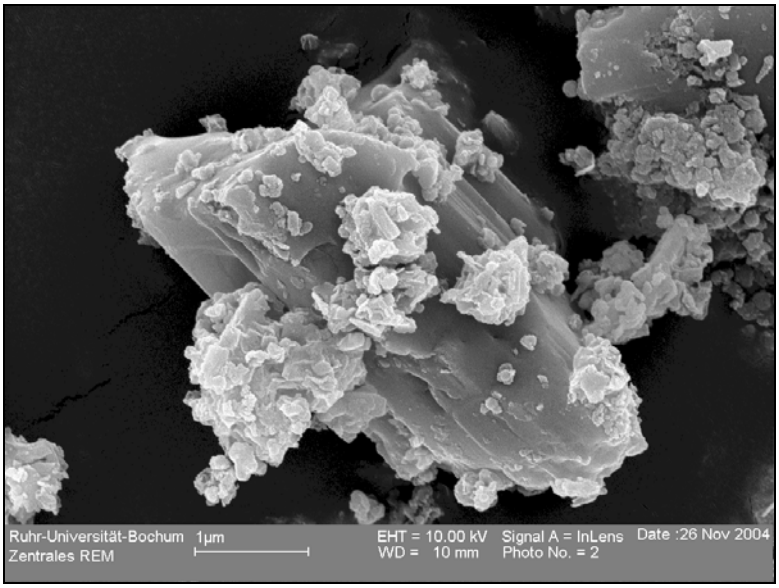

(a)

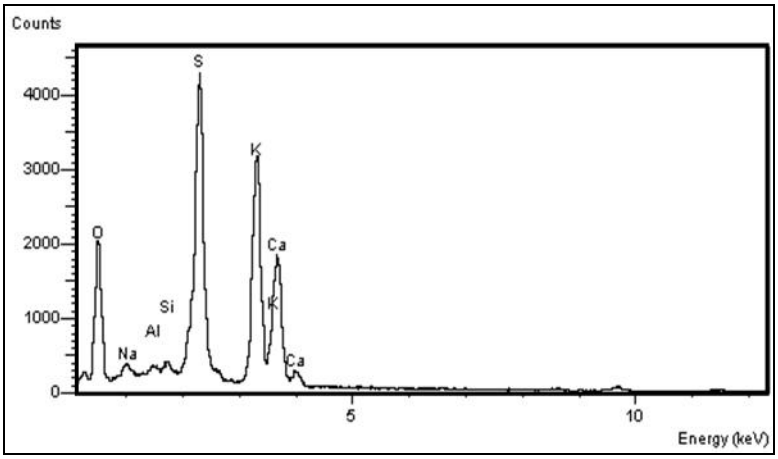

(b)

Figure 4 Main hydrate phases as a result of fly ash solidified with the saturated solution of $Ca(OH)_2$ using ratios of (a) L/S = 3 and (b) L/S = 10 at various times

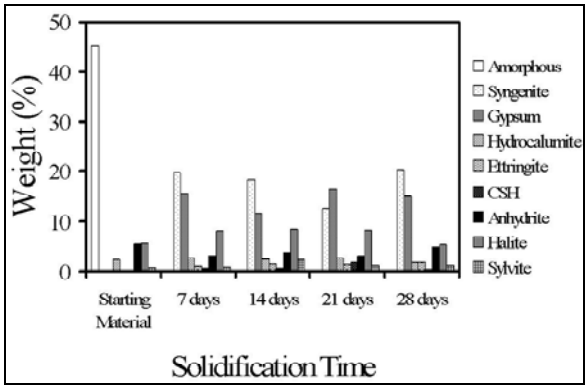

(a)

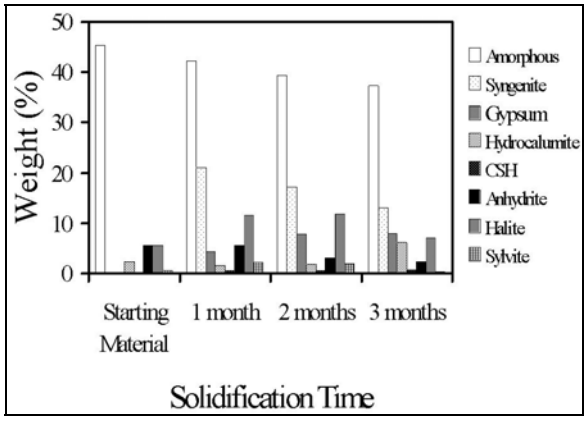

Note: Note that the amorphous phases in the solidified fly ash sample at the L/S ratio of 3 and various times was not detected by the quantitative XRD analysis.

3.3 Formation of hydrated phases during solidification of washed fly ash

Approximately 40 wt. % of the washed fly ash are an amorphous phase; probably silicate glass (Tables 2 and 3). Several phases such as gypsum, ettringite, hydrocalumite, anhydrite and Ca-bearing materials are present in the sample. A small amount of gordaite was also found in the sample. Quartz appeared to be poorly reactive in the saturated $Ca(OH)_2$ solution. Subsequently, mineralogical reactivity in the solidified sample at the L/S mass ratio of 3 as a function of the times was analysed by the XRD Rietveld method [Figure 5(a)]. A dramatic decrease in the content of amorphous phases in the initial seven days was observed just similar to the raw fly ash samples at L/S of 3. Moreover, the content of gypsum increases in the first seven days of solidification, after that the content remains constant with solidification times. The association of the disappearing amorphous phases and the increase of the gypsum content suggested that sulphate compounds reside in amorphous materials, or unstable sulphates are encapsulated in glasses.

Figure 5 Main hydrate phases as a result of pozzolanic solidification of washed fly ash sample with the saturated solution of $Ca(OH)_2$ at (a) L/S = 3 at various times and (b) L/S = 10 at various times

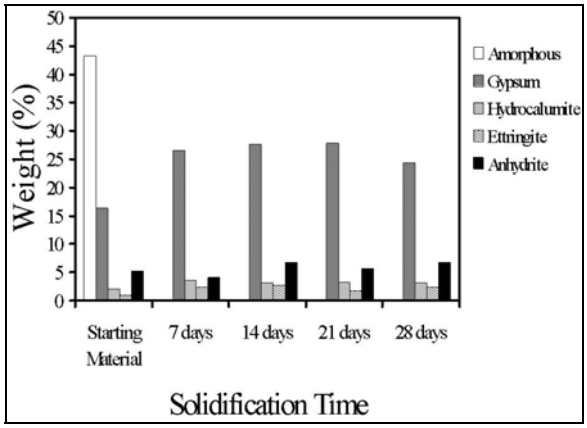

(a)

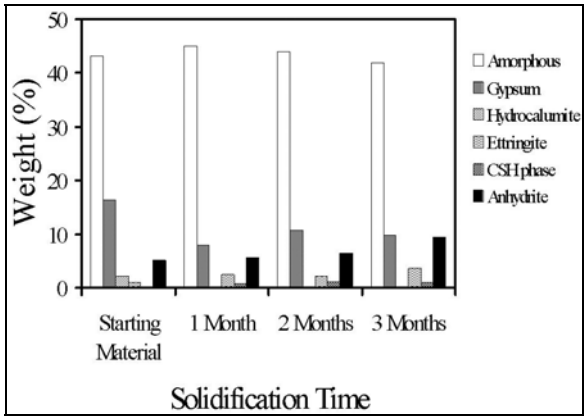

Note: Note that the amorphous phases in the solidified washed fly ash sample at the L/S ratio of 3 and various times was not detected by the quantitative XRD analysis.

Further, the contents of ettringite, hydrocalumite and anhydrite remain constant for beyond seven days. No increase of the hydrate phases was observed, this is probably the usual behaviour of paste having completely solidified at around seven days. Clearly, many of the remaining parent phases such as gehlenite, calcite and portlandite were stable during the pozzolanic reaction, but the disappearance of gordaite was observed.

The change of phases abundance in the solidification of the washed fly ash at the fixed L/S mass ratio of 10 was also determined by the XRD Rietveld method [Figure 5(b)]. All solidified samples contained gypsum as the dominant phases in addition to ettringite, hydrocalumite and C-S-H phase. The formation of ettringite involved a consumption of sulphate at the initial solidification of the paste, and then in the subsequent period, the pozzolanic solidification of the sample produced the C-S-H phase. With increasing times, the production of hydrate phases (ettringite and C-S-H phase) showed a limited increase. This is because of the insufficient availability of aluminates in the sample or the rapid solidification of the pastes. On the other hand, a

considerable quantity of sulphates remained in the solidified samples. This is seen by no marked reduction in the quantity of anhydrite with solidification time. Subsequent pozzolanic solidification of the washed fly ash at the L/S mass ratio of 10 did not modify the glass content of the parent material. The reason for the absence of any marked decrease in the glass content is not obvious, but is probably associated with the formation of protective surface layers over the glass particles through an excess of $Ca(OH)_2$, and subsequently the glass is converted into a not reactive structure.

Figure 6 (a) SEM image of a prismatic morphology of gypsum and (b) EDX spectrum obtained from the washed fly ash solidified with the saturated solution of $Ca(OH)_2$ at the L/S ratio of 10 for 2 months

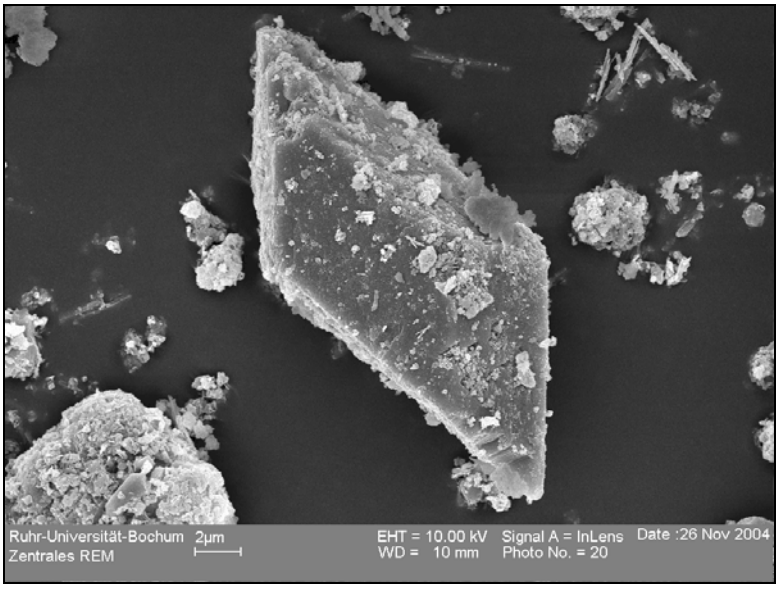

(a)

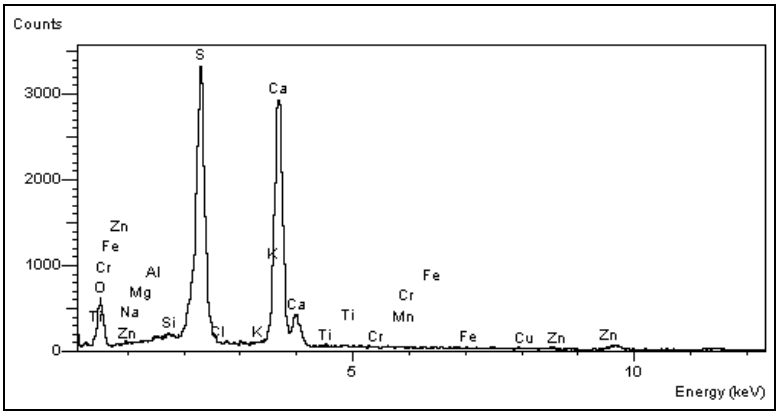

(b)

The finding of gypsum on the solidified washed fly ash after two months at L/S of 10 was confirmed by SEM/EDS analysis, showing prismatic crystals (tablets) with 10–20 μm in diameter and the main elements of S, Ca, and O [Figure 6(a)] are shown, that is similar to the model proposed by Taylor (1990). The small amounts of K, Fe, Al and Si are shown in the EDS spectrum [Figure 6(b)], this may be due to the small grains on the surface of the prism grains.

3.4 Release potential of heavy metals from studied materials

3.4.1 Raw fly ash and its solidified product

The raw fly ash used in this study contains high concentrations of heavy metals, whereas Zn and Pb are abundant (Table 1). Cd, Pb and Zn concentrations in the leaching solution exceeded the US limits (Table 4). Reasonably, the high leaching characteristics of Zn and Pb are probably due to both the Zn and Pb are incorporated in high soluble minerals (e.g., gordaite and caracolite) (Table 2), having a lower chemical resistance in contrast with that of the amorphous phases.

Table 4 Concentrations of heavy metals in the leaching solution after 18-h reaction of leaching process for the fly ash samples and their stabilised products

Sample	*Element*							
	ppm						*ppb*	*pH*
	Cu	*Cd*	*Cr*	*Ni*	*Pb*	*Zn*	*As*	
The raw fly ash	14	12	1	3	17	397	212	5
The solidified sample after 28 days	8	7	<1	<1	11	80	45	5
The washed fly ash	138	35	3	9	393	1504	n.d	5
The solidified washed sample after 28 days	8	22	<1	1	48	386	n.d	6
	ppm							
*U.S. TCLP limits	100	1	5	100	5	5	5	

Note: *US for the TCLP limits

Further Zn-leaching from the fly ash sample is due to the dissolution of ZnCl2. Additionally, the high leaching of Cd is possibly influenced by the solubility-controlling minerals (e.g., $Cd_5(AsO_4)_3Cl$ and $CdCO_3$) as proposed by Eighmy et al. (1995). However, concentrations of Cu, Cr, Ni and As in the leaching solution have passed the TCLP tests. The reasons of the low leachability of those elements are not obvious, but the elements are probably incorporated in the amorphous phase, alloys or oxides, that are insoluble in the acidic solution (Youcai et al., 2002).

The leaching tests of solidified products show that the heavy metals leaching concentrations decrease considerably, in contrast with those from the raw fly ash samples. However, the leaching concentrations of Zn, Pb and Cd do not pass the TCLP limits. The high leachability of these metals may be due to the fact that these metals associated with the chloride minerals and hydrate phases that are obviously leached out during the leaching test. Another explanation of the mobility of metals could be that in the early phase of hardening, bivalent metals can be trapped in the lattice of hydrates and silicates but are replaced by calcium after successive re-crystallisations.

3.4.2 Washed fly ash and its solidified product

The results of TCLP test reveal that, for all washed fly ash samples investigated, the concentrations of some heavy metals (Zn, Pb, Cu and Cd) in the solution exceed the US regulatory limits (Table 4). The high heavy metals leaching of the washed fly ash samples in the solution is also influenced by the high initial contents of the heavy metals during the washing processes (Table 1). It is noted here that As was not detected in the leaching solution.

The leaching behaviour of the washed fly ash samples is explained by recalling that the mobilisation of the particular heavy metal (Zn, Pb and Cd) is influenced by the stability of hydrate phases (i.e., ettringite and hydrocalumite). Ettringite and hydrocalumite are probably soluble phases controlling leaching of particularly Cd^{2+}, Pb^{2+}, and Zn^{2+}-ions at the pH values examined (Rémond et al., 2002; Taylor, 1990). However, the concentrations of Cr and Ni in the leachate are below the limits, suggesting that these elements may be distributed in the amorphous phase, alloys (Fe-Cr-Ni) or spinel that becomes less soluble in acid.

Further mobility of heavy metals from the washed fly ash is considerably reduced by pozzolanic solidification (Table 4). On the other hand, the leaching concentration of Zn from all solidified samples does not pass the limits. It is presumable that a large amount of Zn was concentrated in the most unstable phases of ettringite, as confirmed by SEM/EDS analysis. Hence, the high leaching property of Zn is simply explained by the poorer leaching resistance of ettringite, or smaller quantities of Zn and Pb are fixed in the amorphous C-S-H phases (Taylor, 1990). However, the concentrations of Ni and Cr in the leaching solution are well below the limits. These elements should be mainly present in the solidified samples as likely amorphous C-S-H phases, spinel or alloys with low leachability. Nevertheless, the pozzolanic solidification of some washed fly ash samples is ineffective for immobilising all heavy metals examined.

4 Discussion

The presented results of pozzolanic solidification experiments of the raw and washed fly ashes in the saturated solution of $Ca(OH)_2$ confirmed that the solidified products are formed possessing cementitious properties. The $Ca(OH)_2$ solution plays an important role as an activator, providing portlandite to react with the active Al and Si-ions that were liberated from the glassy substance. It also acts as a cementitious agent by producing highly alkaline conditions, in which silica and alumina dissolve into solution and react with the available calcium to form pozzolanic products, thereby increasing strength, impermeability and durability of the solidified product to chemical attack (Aubert et al., 2006). The overall pozzolanic solidification is greatly slowed. Here portlandite is an unstable phase under atmospheric conditions and evolves by reaction with the atmospheric CO_2 into a stable calcium carbonate phase (e.g., calcite). The hydrated calcium carbonate may be directly precipitated during the solidification. The progress of the pozzolanic reaction was investigated by recording new-formed minerals and changes in the relative amounts of glassy phase in the XRD Rietveld data. The results show that the reactivity of glassy phase with calcium hydroxide determines the pozzolanic activity of the raw and washed fly ashes which is controlled by the L/S ratio. Therefore fly ash can be considered pozzolanic material. However, some questions are still open, namely in

order to know its reactivity, e.g., why a certain fly ash reacts faster than others, what type of fly ash can be used as pozzolans, what amounts of fly ash needed to achieve optimisation. In order to measure the reactivity of fly ash used in mortars and concretes, several methods should be studied for measuring and studying different aspects of the lime/fly ash and cement/fly ash reaction, such as compression strength, reaction kinetics and lime consumption.

Moreover, the mineralogical composition and amorphous phases of the raw fly ash samples were obviously changed, while amorphous phases provide an important source of sulphate, that subsequently interacts with the $Ca(OH)_2$ solution to produce gypsum and syngenite. The pozzolanic reaction also probably causes partial conversion of the soluble anhydrite into gypsum, while the anhydrite-gypsum transition leads to a volume expansion of x 1.60, making this solidified material less suitable for such building purposes where cracking and expansion cannot be tolerated. As a result of the reaction, the quantity of anhydrite was not reduced, corresponding to the formation of gypsum, whereas an amorphous calsium sulphate was hydrated into syngenite. During the solidification process, the large quantity of gypsum was initially formed, but once the soluble sulphates within the pastes were exhausted, subsequent reaction of gypsum and K_2SO_4 resulted in the formation of syngenite. Thus, the syngenite forming reactions are represented as follows:

$$K_2SO_4 + CaSO_4 \cdot 2H_2O \Rightarrow K_2Ca\,(SO_4)_2 \cdot H_2O + H_2O \quad (1)$$

In the present study, the crystalline form of arcanite (K_2SO_4) was not be detected by XRD in any fly ash sample; therefore the amorphous K_2SO_4 phases have probably contributed to the formation of syngenite. Subsequently syngenite appears to be much more abundant after 28 days of solidification using the smaller L/S mass ratios (< 3).

Further, this paper has not attempted to deal with the pozzolanic reaction fly ash-$Ca(OH)_2$ with saturated water solution of lime at wide variation of L/S ratio. This reaction is principally limited by the rate of the chemical reaction taking place on the phase boundary of glass phase with the lime solution. In the L/S ratio of 3, the glass content in the raw and washed fly ashes are considered sufficiently high to influence the pozzolanic reaction. However, work remains to be carried out to investigate the behaviour of glass phase at wide variation of L/S ratio with the lime solution.

The additional important secondary Ca-phase in the solidified fly ash is hydrocalumite, that forms by the reaction of CaO and Al_2O_3 at pH range of 10–11. The limiting components of this reaction are the amount of Al_2O_3 in the fly ash that remained unused during the formation of hydrocalumite. Perhaps, the aluminous reagent is not oxide but aluminate ion used for this mineral formation. The composition of obtained hydrocalumite seems to vary considerably depending on the advancement of solidification processes. Here, hydrocalumite is probably represented as $4CaO{\cdot}Al_2O_3{\cdot}12H_2O$ with some CO_3^{2-} and a monoclinic crystal structure, the composition of that is similar to α-$3CaO{\cdot}Al_2O_3{\cdot}CaCl_2{\cdot}10H_2O$. Also many synthetic members of hydrocalumite are reported in the literature, some of them belong to the solid solution series $3CaO{\cdot}Al_2O_3{\cdot}CaCl_2{\cdot}10H_2O$-$4CaO{\cdot}Al_2O_3{\cdot}13H_2O$ (Taylor, 1990). Hydrocalumite is an anionic exchanger able to trap metallic oxyanions (e.g., CrO_4--) in its anion exchange capacity. The real formula of hydrocalumite mineral is $Ca(3\text{-}x)Alx(OH)_6$. x/n AnN- pH_2O where Ann- is a compensating anion of valence n. In the present study, hydrocalumite formation is not directly applied to chloride binding mechanisms; this is

due to the fact that the content in alkali chlorides in the raw (halite and sylvite) and washed fly ash remained unchanged. Additionally the amount of hydrocalumite is unchanged with the advancement of pozzolanic solidification.

Other important hydrated phases found during pozzolanic solidification is ettringite, that results from a reaction of calcium hydroxide, aluminium oxide and gypsum/anhydrite according to the following reaction:

$$Al_2O_3 + 3Ca(OH)_2 + 3CaSO_4 + 29H_2O \Rightarrow 3CaO \cdot Al_2O_3 \cdot 3CaSO_4 \cdot 32H_2O \quad (2)$$

Here, the formation of ettringite was not favoured under low alkaline condition of the fly ash samples examined (pH values ranging from 10 to 11). This feature is also attributed to the insufficient content of aluminate phases in some fly ash samples to react with sulphate. Another reason for the absence of Al_2O_3 is that the aluminous reagent could be not oxide but aluminate ion. The presence of heavy metals (Pb and Zn) from the fly ash, in solution, possibly interfered with the equilibrium of calcium for the ettringite formation (Glasser, 1997). The crystallisation of ettringite also causes to a volume expansion of x3. Moreover, the remaining phases of solidified fly ash identified are amorphous C-S-H gel or another amorphous phase. The formation of C-S-H phases is probably because of a pozzolanic or latent hydraulic reaction in combination with $Ca(OH)_2$ according to the following reaction:

$$SiO_2 + Ca(OH)_2 + H_2O \Rightarrow \text{C-S-H} \quad (3)$$

However, the quantity of C-S-H formed in the particular types of samples (the raw and the washed fly ash samples) is extremely low; this is probably due to the inappropriate quantity of $Ca(OH)_2$ present in the solution, while the amorphous silica in the fly ash may not react with the hydrated lime to form calcium silicate hydrates ($xCaO.SiO_2.yH_2O$).

With regards to the washed fly ash samples that are characterised by the low contents of sylvite and halite, the formation of ettringite during treatments with saturated solution of $Ca(OH)_2$ began after some days and with slower development. Apparently, the saturated $Ca(OH)_2$ solution did not favour to the attack of the glass particles, and then provided not much of the aluminate phases to react with the whole sulphate for ettringite formation (Ubbriaco and Calabrese, 2000; Ubbriaco et al., 2001). It has been reported previously by Ubbriaco et al. (2001) that the excess of $Ca(OH)_2$ has a strong influence on the formation of ettringite including C-S-H. Thus, the mass ratio of fly ash/lime-water is an area of concern about the paste preparation for the development of ettringite and C-S-H phase. In contrast, a rapid development of gypsum was observed, whereas anhydrite was not altered by the pozzolanic reaction. Further, a moderate quantity of gordaite was also noticed in some solidified products, because a small quantity of chloride still remained in the materials contributing to the formation of this phase.

The pozzolanic solidification of the raw and the washed fly ash samples had a positive influence on the reduced leaching of metals, though some metals (Cd, Pb and Zn) still exceeded the TCLP limits. The reduction in mobilisation of heavy metals examined is caused by the incorporation of metals into secondary phases with low solubility. For example, Cd, Pb and Zn are possibly incorporated in the C-S-H phases and in carbonates such as calcite that is quite abundant in the sample.

The leaching behaviour of these metals in the solidified waste products are mainly controlled by the alkaline nature and acid buffering capacity of the solidified and stabilised (S/S) matrices (Li et al., 2001). A number of studies proved that the

leachability of metals (Cd, Cu, Pb and Zn) in waste materials is controlled by the solubility of metal compounds in the leachate (Johnson et al., 1996; Yvon et al., 2006). The leaching of Cd may be controlled by precipitation of carbonate of $CdCO_3$, as proposed by Eighmy et al. (1995). The highly alkaline condition of the solidified matrix leads most of these metals to exist as metal hydrated phases, metal hydroxides and calcium-metal compounds (Li et al., 2001). Cu may also exist as hydroxides or react with calcium to form complex compounds in the S/S waste materials. Zinc is expected to form hydroxides in the high pH condition (pH > 8) of the fly ash-$Ca(OH)_2$ system. Zinc hydroxide, a typical amphoteric hydroxide functions as both an acid and a base. The equilibrium can be expressed as follow:

$$Zn^{2+} + 2OH^- \rightarrow Zn(OH)_2 \rightarrow 2H^+ \rightarrow ZnO_2^{2-} \quad (4)$$

Here the hydroxy-complexes $Zn(OH)_4^{2-}$ and $Zn(OH)_5^{3-}$ can be present in a strong alkaline solution. Their anionic properties prevent their adsorption onto the negative surface of the C-S-H, but they may form the calcium zinc complex hydrated compound $CaZn_2(OH)_6 \bullet H_2O$ with Ca. Moreover, the dissolved species in solution for lead are Pb^{2+}, $PbOH^+$, $Pb(OH)2^0$, and $Pb(OH)3^-$. At low pH condition, $PbOH^+$ is the dominant dissolved Pb(II) species, but with the increase of pH, Pb can form hydroxide precipitate and then become the more insoluble PbO.

In the case of metal oxyanions (As and Cr), the mobility of those metals is supposed to be mainly controlled by dissolution/precipitation reactions in neutral to alkaline systems (Cornelis et al., 2008; Quina et al., 2009). Here Ca metallates may control the solubility of oxyanions in the oxidised form as As^V, As^{III} and Cr^{VI}. Moreover, Cr in fly ash may be incorporated into the stable spinel matrix (Eighmy et al., 1995); and could be slowly release out only if the glass phases and Fe-Mn oxide have been dissolved. Therefore Cr is almost totally present in the extracted samples. Similar to Cr, dissolution/precipitation of $Ni(OH)_2$ can describe the leaching behaviour of Ni at pH 7–14. But the surface adsorption reaction may play an important role of Ni leaching at pH 4–8.

Further, the pozzolanic solidification of raw and washed fly ashes could be an environmentally safe solution to the problem of heavy metal leaching, if these ashes could be properly prepared by extracting the heavy metals to some extent with chemical agents as proposed by Youcai et al. (2002). From the economic point of view, the cost for pozzolanic solidification and extraction process is suggested to be relatively lower in contrast with that for high temperature volatilisation and evaporation of heavy metals or vitrification (ISWA, 2008). However, additional studies should be carried out to examine the long-term stability of the solidification matrix. This next procedure becomes important to enhance the possibility of reuse of fly ash as a valuable resource.

5 Conclusions

The pozzolanic solidification experiments of the raw and washed fly ashes in the saturated solution of $Ca(OH)_2$ formed solid materials possessing cementitious properties. The considerable formation of gypsum and syngenite, but small amounts of ettringite, hydrocalumite and C-S-H phases (modelled by tobermorite-14 Å) were produced in the solidified raw and washed fly ashes. Specifically, the high content of amorphous phases

in the raw fly ash is an important source of Ca and SO4 interacting with aluminates to form ettringite, whereas the formation of hydrocalumite is possible the interaction of calcium hydroxide and aluminates. In addition, gypsum was the dominant hydrated phases formed in the solidified washed fly ash. A dramatic reduction in the heavy metal leaching from the fly ash sample is achieved by pozzolanic solidification, although concentrations of some metals (Cd, Pb and Zn) in the leaching solution do not meet the US-TCLP limits. Finally, these experimental results provide valuable data for the development of fly ash processing strategy with economic advantages and environmental benefits.

Acknowledgements

The authors wish to thank Dr. Neuser for their help in collecting electron microscope analysis data. Special thank to Dr. Reinecke for his support in the XRD laboratory. The assistance of Hendrik Narjes, Astrid Michele and Sandra Grabowski performing laboratory experiments is also gratefully acknowledged. Thanks to MVA Iserlohn, Germany for providing the fly ash sample, and the Katholischer Akademischer Austausch Dienst (KAAD) Bonn, Germany for supporting the study. We gratefully acknowledge the reviewers for their time and efforts in reviewing of our paper.

References

ACI 116R (2000) American Concrete Institute (ACI), Cement and Concrete Terminology, Farmington Hills, MI, USA.

Akiko, K., Yukio, N. and Teruji, I. (1996) 'Chemical speciation and leaching properties of elements in municipal incineration ashes', *Waste Management*, Vol. 16, Nos. 5–6, pp.523–536.

Alba, N., Vazquez, E., Gasso, S. and Baldasano, J. M. (2001) 'Stabilization/solidifcation of MSW incineration residues from facilities with different air pollution control systems. Durability of matrices versus carbonation', *Waste Management*, Vol. 21, No. 4, pp.313–323.

Aubert, J.E., Husson, B. and Sarramone, N. (2006) 'Utilization of municipal solid waste incineration (MSWI) fly ash in blended cement. Part 1: processing and characterization of MSWI fly ash', *Journal of Hazardous Materials*, Vol. 136, No. 3, pp.624–631.

Aubert, J.E., Husson, B. and Sarramone, N. (2007) 'Utilization of municipal solid waste incineration (MSWI) fly ash in blended cement. Part 2. Mechanical strength of mortars and environmental impact', *Journal of Hazardous Materials*, Vol. 146, Nos. 1–2, pp.12–19.

Bayuseno, A.P. (2006) *Mineral Phases in Raw and Processed Municipal Waste Incineration Residues – Towards a Chemical Stabilisation and Fixation of Heavy Metals*, PhD Thesis, Ruhr-Universität Bochum, Germany.

Bertolini, L., Carsana, M., Cassago, D., Cursio, A.Q. and Collepardi, M. (2004) 'MSWI ashes as mineral additions in concrete', *Cement and Concrete Research*, Vol. 34, No. 10, pp.1899–1906.

Chen, Q.Y., Tyrer, M., Hills, C.D., Yang, X.M. and Carey, P. (2009) 'Immobilisation of heavy metal in cement-based solidification/stabilisation: a review', *Waste Management*, Vol. 29, No. 1, pp.390–403.

Cornelis, G., Johnson, C.A., Van Gerven, T. and Vandecasteele, C. (2008) 'Leaching mechanisms of oxyanionic metalloid and metal species in alkaline solid wastes: a review', *Applied Geochemistry*, Vol. 23, No. 5, pp.955–976.

Deer, W.A., Howie, R.A. and Zussman, J. (1996) *An Introduction to the Rock Forming Minerals*, Longman Group Limited, London.

Eighmy, T., Eusden, J.D., Krzanowski, J.E., Dominggo, D.S., Stampfli, D., Martin, J. and Erickson, P.M. (1995) 'Comprehensive approach toward understanding element speciation and leaching behavior in municipal solid waste incineration electrostatic precipitator ash', *Environmental Science and Technology*, Vol. 29, No. 3, pp.629–646.

Erol, M., Kücükbayrak, S., Ersoy-Mericboyu, A. and Övecoglu, M.L. (2001) 'Crystallization behaviour of glasses produced from fly ash', *Journal of the European Ceramic Society*, Vol. 21, No. 16, pp.2835–2841.

Ferreira, C., Ribeiro, A. and Ottosen, L. (2003) 'Possible applications for municipal solid waste fly ash', *Journal of Hazardous Materials*, Vol. 96, Nos. 2–3, pp.201–216.

Glasser, F.P. (1997) 'Fundamental aspects of cement solidification and stabilization', *Journal of Hazardous Materials*, Vol. 52, Nos. 2–3, pp.151–170.

Hill, R.J. and Howard, C.J. (1987) 'Quantitative phase analysis from neutron powder diffraction data using the Rietveld method', *Journal of Applied Crystallography*, Vol. 20, Part 6, pp.467–474.

Hjelmar, O. (1996) 'Disposal strategies for municipal solid waste incineration residues', *Journal of Hzardous Materials*, Vol. 47, Nos. 1–3, pp.345–368.

Hong, K.J., Tokunaga, S. and Kajiuchi, T. (2000a) 'Extraction of heavy metals from MSW incinerator fly ashes by chelating agents', *Journal of Hazardous Materials*, Vol. 75, No. 1, pp.57–73.

Hong, K.J., Tokunaga, S., Ishigami, Y. and Kajiuchi, T. (2000b) 'Extraction of heavy metals from MSW incinerator fly ash using saponins', *Chemosphere*, Vol. 41, No. 3, pp.345–352.

Inorganic Crystal Structure Database (ICSD) (1999) FIZ Karlsruhe and the GMELIN Institute, Frankfurt, Eggenstein-Leopoldshafen. Germany.

ISWA (2008) *Management of APC Residues from W-T-E Plants – An Overview of Management Options and Treatment Methods*, ISWA-Working Group on Thermal Treatment of Waste, Subgroup APC Residues from W-T-E Plants.

Johnson, C.A., Kersten, M., Ziegler, F. and Moor, H.C. (1996) 'Leaching behaviour and solubility-controlling solid phases of heavy metals in municipal solid waste incinerator ash', *Waste Management*, Vol. 16, Nos. 1–3, pp.129–134.

Katsuura, H., Inoue, T., Hiraoka, M. and Sakai, S. (1996) 'Full-scale plant study on fly ash treatment by the acid extraction process', *Waste Management*, Vol. 16, Nos. 5–6, pp.491–499.

Le Forestier, L.L. and Libourel, G. (1998) 'Characterization of flue gas residues from municipal solid waste combustors', *Environmental Science and Technology*, Vol. 32, No. 15, pp.2250–2256.

Li, X.D., Poon, C.S., Sun, H., Lo, I.M.C. and Kirk, D.W. (2001) 'Heavy metal speciation and leaching behaviors in cement based solidified/stabilized waste materials', *Journal of Hazardous Materials*, Vol. 82, No. 3, pp.215–230.

Mahieux, P.Y., Aubert, J.E., Cyr, M., Coutand, M. and Husson, B. (2010) 'Quantitative mineralogical composition of complex mineral wastes-contribution of the Rietveld method', *Waste Management*, Vol. 30, No. 3, pp.378–388.

Malviya, R. and Chaudhary, R. (2006) 'Leaching behavior and immobilization of heavy metals in solidified/stabilized products', *Journal of Hazardous Materials*, Vol. 137, No. 1, pp.207–217.

Mangialardi, T. (2003) 'Disposal of MSWI fly ash through a combined washing-immobilisation process', *Journal of Hazardous Materials*, Vol. 98, Nos. 1–3, pp.225–240.

Mangialardi, T., Paolini, A.E., Polettini, A. and Sirini, P. (1999) 'Optimization of the solidification/stabilization process of MSW fly ash in cementitious matrices', *Journal of Hazardous Materials*, Vol. 70, Nos. 1–2, pp.53–70.

Mulder, E. (1996) 'Pre-treatment of MSWI fly ash for useful application', *Waste Management*, Vol. 16, Nos. 1–3, pp.181–184.

Pan, J.R., Huang, C., Kuo, J.J. and Lin, S.H. (2008) 'Recycling MSWI bottom ash and fly ash as raw materials for Portland cement', *Waste Management*, Vol. 28, No. 7, pp.1113–1118.

Park, Y.J. and Heo, J. (2002) 'Vitrification of fly ash from municipal solid waste incinerator', *Journal of Hazardous Materials*, Vol. 91, Nos. 1–3, pp.83–93.

Polettini, A., Pomi, R., Trinci, L., Muntoni, A. and Lo Mastro, S. (2004) 'Engineering and environmental properties of thermally treated mixtures containing MSWI fly ash and low-cost additives', *Chemosphere*, Vol. 56, No. 10, pp.901–910.

Pouchou, J.L. and Pichoir, J.F. (1991) 'Quantitative analysis of homogeneous or stratified micro-volume applying the model 'PAP'', in Heinrich, K.F.S. and Newbeury, D.E. (Eds.): *Electron Probe Quantition*, Plenum Press, New York.

Quina, M.J., Bordado, J.C. and Quinta-Ferreira, R.M. (2008) 'Treatment and use of air pollution control residues from MSW incineration: an overview', *Waste Management*, Vol. 28, No. 11, pp.2097–2121.

Quina, M.J., Bordado, J.C.M and Quinta-Ferreira, R.M. (2009) 'The influence of pH on the leaching behaviour of inorganic components from municipal solid waste APC residues', *Waste Management*, Vol. 29, No. 9, pp.2483–2493.

Rémond, S., Bentz, D.P. and Pimienta, P. (2002) 'Effects of the incorporation of municipal solid waste incineration fly ash in cement pastes and mortars II: modelling', *Cement and Concrete Research*, Vol. 32, No. 4, pp.565–576.

Rietveld, H.M. (1969) 'A profile refinement method for nuclear and magnetic structures', *Journal of Applied Crystallography*, Vol. 2, Part 2, pp.65–71.

Sabbas, T., Polettini, A., Pomi, R., Astrup, T., Hjelmar, O., Mostbauer, P., Cappai, G., Magel, G., Salhofer, S., Speiser, C., Heuss-Assbicher, S., Klein, R. and Lehner, P. (2003) 'Management of municipal solid waste incineration residues', *Waste Management*, Vol. 23, No. 1, pp.61–88.

SIROQUANT (2002) *Quantitative XRD Phase Analysis Software Based on the Rietveld Method*, Version 2.5, CSIRO, Australia.

SØrensen, M.A., Koch, B.C., Stackpoole, M.M., Bordia, R.K., Benjamin, M.M. and Christensen, T.H. (2000) 'Effects of thermal treatment on mineralogy and heavy metal behaviour in iron oxide stabilized air pollution control residues', *Environmental Science and Technology*, Vol. 34, No. 21, pp.4620–4627.

Taylor, H.F.W. (1990) *Cement Chemistry*, Academic Press, London and New York.

U.S. EPA (1990) *Part 261, Appendix II-Method 1311 Toxicity Characteristic Leaching Procedure (TCLP)*, Federal Register, Vol. 55, No. 61, March 29, 1990, Rules and Regulations, 1990, pp.11863–11877.

Ubbriaco, P. and Calabrese, D. (2000) 'Hydration behaviour of mixtures of cement and fly ash with high sulphate and chloride content', *Journal of Thermal Analysis and Calorimetry*, Vol. 61, No. 2, pp.615–623.

Ubbriaco, P., Bruno, P., Traini, A. and Calabrese, D. (2001) 'Fly ash reactivity: formation of hydrate phases', *Journal of Thermal Analysis and Calorimetry*, Vol. 66, No. 1, pp.293–305.

Walker, R. and Pavıa, S. (2011) 'Physical properties and reactivity of pozzolans, and their influence on the properties of lime-pozzolan pastes', *Materials and Structures*, Vol. 44, No. 6, pp.1139–1150.

Wang, K.S., Chiang, K.Y., Lin, K.L. and Sun, C.J. (2001) 'Effects of a water-extraction process on heavy metal behaviour in municipal solid waste incinerator fly ash', *Hydrometallurgy*, Vol. 62, No. 2, pp.73–81.

Williams, P.J., Biernacki, J.J., Walker, L.R., Meyer, H.M., Rawn, C.J. and Bai, J. (2002) 'Microanalysis of alkali-activated fly ash-CH pastes', *Cement and Concrete Research*, Vol. 32, No. 6, pp.963–972.

Youcai, Z., Song, L. and Guojian, L. (2002) 'Chemical stabilization of MSW incinerator fly ashes', *Journal of Hazardous Materials*, Vol. 95, Nos. 1–2, pp.47–63.

Yvon, J., Antenucci, D., Jdid, E.A., Lorenzi, G., Dutre, V., Leclerq, D., Nielsen. P. and Veschkens, M. (2006) 'Long-term stability in landfills of municipal solid waste incineration fly ashes solidified/stabilized by hydraulic binders', *Journal of Geochemical Exploration*, Vol. 90, Nos. 1–2, pp.143–155.

Yvon, J., Antenucci, D., Jdid, E.A., Lorenzi, G., Leclerq, D., Dutre, V. and Nielsen, P. (2008) 'Solidified/stabilized municipal solid waste incineration fly ashes in cement based matrix: aluminium hydrolysis effect upon lead speciation in solids', Lehmann, E.C. (Ed.): *Landfill Research Focus*, pp.293–310, Nova Science Publishers, New York.